Chinese Chemical Letters 36 (2025) 110351

Contents lists available at ScienceDirect

Chinese Chemical Letters

journal homepage: www.elsevier.com/locate/cclet

Plasma metabolomics combined with mass spectrometry imaging reveals crosstalk between tumor and plasma in gastric cancer genesis and metastasis

Yanhua Chen[a,e,f,1], Xian Ding[b,h,1], Jun Zhou[c,1], Zhaoying Wang[a,e], Yunhai Bo[d], Ying Hu[g], Qingce Zang[b], Jing Xu[b], Ruiping Zhang[b], Jiuming He[b], Fen Yang[d,*], Zeper Abliz[b,*]

[a] Key Laboratory of Mass Spectrometry Imaging and Metabolomics (State Ethnic Affairs Commission), Center for Imaging and Systems Biology, College of Life and Environmental Sciences, Minzu University of China, Beijing 100081, China
[b] State Key Laboratory of Bioactive Substance and Function of Natural Medicines, Institute of Materia Medica, Chinese Academy of Medical Sciences, Peking Union Medical College, Beijing 100050, China
[c] Key Laboratory of Carcinogenesis and Translational Research (Ministry of Education/Beijing), Department of Gastrointestinal Oncology, Peking University Cancer Hospital & Institute, Beijing 100142, China
[d] Key Laboratory of Carcinogenesis and Translational Research (Ministry of Education), Center of Drug Clinical Trial, Peking University Cancer Hospital and Institute, Beijing 100142, China
[e] Beijing Engineering Research Center of Food Environment and Public Health, Minzu University of China, Beijing 100081, China
[f] Key laboratory of Ethnomedicine of Ministry of Education, School of Pharmacy, Minzu University of China, Beijing 100081, China
[g] Key Laboratory of Carcinogenesis and Translational Research (Ministry of Education), Department of BioBank, Peking University Cancer Hospital and Institute, Beijing 100142, China
[h] Pharmacy Department of Beijing Chao–Yang Hospital, Capital Medical University, Beijing 100020, China

ARTICLE INFO

Article history:
Received 22 April 2024
Revised 19 July 2024
Accepted 20 August 2024
Available online 20 August 2024

Keywords:
Metabolomics
Spatial-resolved metabolomics
Gastric cancer
Blood-tumor metabolic crosstalk
Lipid peroxidation

ABSTRACT

Gastric Carcinoma (GC) is a highly fatal malignant tumor with a poor prognosis. Its elevated mortality rates are primarily due to its proclivity for late-stage metastasis. Exploring the metabolic interactions between tumor microenvironment and the systemic bloodstream could help to clearly understand the mechanisms and identify precise biomarkers of tumor growth, proliferation, and metastasis. In this study, an integrative approach that combines plasma metabolomics with mass spectrometry imaging of tumor tissue was developed to investigate the global metabolic landscape of GC tumorigenesis and metastasis. The results showed that the oxidized glutathione to glutathione ratio (GSSH/GSH) became increased in non-distal metastatic GC (M0), which means an accumulation of oxidative stress in tumor tissues. Furthermore, it was found that the peroxidation of polyunsaturated fatty acids, such as 9,10-EpOMe, 9-HOTrE, *etc*., were accelerated in both plasma and tumor tissues of distal metastatic GC (M1). These changes were further confirmed the potential effect of CYP2E1 and GGT1 in metastatic potential of GC by mass spectrometry imaging (MSI) and immunohistochemistry (IHC). Collectively, our findings reveal the integrated multidimensional metabolomics approach is a clinical useful method to unravel the blood-tumor metabolic crosstalk, illuminate reprogrammed metabolic networks, and provide reliable circulating biomarkers.

Gastric carcinoma (GC), an aggressive malignancy of the gastric mucosal epithelium, had global incidence and mortality rates of over 1 million and 0.77 billion in 2020, respectively [1]. Projections indicate that by 2040, the GC incidence and mortality rates will signify a substantial increase of about 63% and 66% [2]. Most patients are found with locally advanced or metastatic GC (stage IV) at diagnosis, making metastasis a significant obstacle to clinical GC management [3,4]. Furthermore, 50% to 70% of patients who undergo radical resection are at risk of metastatic recurrence [3], resulting in a poor prognosis with a 5-year survival rate of <30% [5]. Consequently, early detection of GC and its metastasis, along with effective therapeutic strategies, holds immense importance in enhancing patients' survival outcomes. As opposed to treatable primary tumors, metastatic GC is a systemic ailment. Therefore, comprehensive molecular analysis of metastatic tumors

* Corresponding authors.
E-mail addresses: yf7854@163.com (F. Yang), zeper@imm.ac.cn (Z. Abliz).
[1] These authors contributed equally to this work.

https://doi.org/10.1016/j.cclet.2024.110351
1001-8417/

is necessary to systemically manage and treat metastatic cancer [6]. Metabolomics has significantly enhanced our understanding of metabolic reprogramming in the context of cancer progression [7-10]. A study that integrated metabolomics and transcriptomics revealed elevated fructose levels and reduced oxygen levels in liver metastasis colorectal cancer models [7]. A targeted metabolomics study [8] revealed the accumulation of methylmalonic acid (MMA) in old donors' serum, and it potentially induced SOX4 expression, resulting in transcriptional reprogramming and enhancing the aggressiveness of cancer cells. Recently, machine learning-based metabolomics have revealed the metabolic landscape of GC and identify two distinct biomarker panels that enable early detection and prognosis prediction respectively, thus facilitating precision medicine in GC [9].

Metabolic reprogramming is one of the characteristic features of cancer onset and advancement [11]. Elucidating tumor metabolic phenotypes and exploiting their metabolic susceptibilities offers novel insights into resistant cancer diagnosis, prognosis, and precise therapeutic intervention [6,12]. Blood detection is a significant non-invasive approach for cancer diagnosis, treatment, and prognostic assessment. However, small-molecule metabolites may be diluted or biologically transformed when released from the primary tumor into the bloodstream, lowering the diagnostic and prognostic efficacy. Tumor tissues possess substantial gene mutation and metabolic reprogramming data, which could be useful in cancer diagnosis and prognosis [13]. Spatially-resolved metabolomics offers a comprehensive spatio-temporal perspective on body, tissue, or cell metabolism, enabling the effective assessment of the metabolic heterogeneity that drives tumorigenesis and metastasis [14]. He *et al.* [15] developed an enhanced mass spectrometry imaging (MSI) method by air-flow assisted desorption electrospray ionization (AFADESI) to obtain some differential metabolites showing gradual changing trend from normal to adjacent to cancerous areas. Moreover, it is a valuable research method for investigating metabolic crosstalk interactions between the tumor microenvironment (TME) and various cells or organs. Therefore, a comprehensive analysis of metabolomics and their spatial characteristics in blood and tumor tissues is critical for elucidating the underlying mechanisms of disease progression and facilitating the precise detection of circulating tumor markers.

An integrative metabolomics approach that combines LC–MS-based metabolomics with MSI-based spatially-resolved metabolomics was proposed to depict the global metabolomic landscape of plasma and primary tissues during GC progression from tumorigenesis to metastasis.

A total of 254 participants (59 healthy volunteers (HC), 50 non-distal metastatic GC patients (M0), and 145 distal metastatic GC patients (M1)) were enrolled in the study. Table S1 (Supporting information) shows basic characteristics of the study cohort. Intraoperative tissue samples were obtained from 15 patients ($n = 6$, M0; $n = 5$, M1) and 15 *para*-cancerous tissue samples, as shown in Fig. S1B (Supporting information). The detailed electronic medical record (EMR) of 136 GC patients [$n = 29$, M0; $n = 107$, M1] were summarized in Figs. S1C and S2 (Supporting information). The plasma and tissue samples were collected at Beijing Cancer Hospital. The Ethics Committee of Peking University Cancer Hospital approved this study (Approval Number: 2016KT57), and each patient provided informed consent before sample collection.

LC–MS/MS-based metabolomics analysis was performed on 254 plasma samples. Detailed sample pre-processing procedures and LC–MS analysis parameters were as described in previously reported work [16]. Spatially-resolved metabolomics analysis was performed on an AFADESI-MSI platform [17] along with a Q-orbitrap spectrometry system (Q Exactive, Thermo Scientific, USA). The detailed experimental materials are in "Materials and Methods" in Supporting information.

The quality control (QC) and wide-coverage metabolite identification were firstly performed for a thorough coverage of plasma metabolome. The QC assessment results demonstrated that the stability of the LC–MS/MS and AFADESI-MSI platforms was acceptable, ensuring the reproducibility and reliability of the data (Fig. S3 in Supporting information). We identified 397 metabolites (tissue samples) and 655 metabolites (plasma samples) using the in-house standard database and the public databases (Figs. S1D and E in Supporting information), involving in biochemical reactions of 42 and 86 significant metabolic pathways, respectively (hits >2 & $P < 0.05$). This outcome indicates sufficient pathway coverage to interpret metabolic changes in GC patients' tissue and plasma samples (Fig. S4 in Supporting information).

The discernible trend of progressive metabolic changes was observed in the plasma metabolic expression profiles of HC, M0, and M1, as shown by partial least squares discriminant analysis (PLS-DA) (Fig. 1A) and the Euclidean distance measuring analysis of the metabolic profiles (Fig. 1A). Two-hundred and sixty-four metabolites exhibited significant alterations in plasma (Fig. 1B and Fig. S5A in Supporting information). Specifically, 164 metabolites were significantly elevated or decreased in M0 patients' plasma, while 239 metabolites experienced changes in M1 patients. The discriminated metabolites could be categorized into 13 classes based on their structural and functional characteristics. The results indicated that fatty acids (FAs), steroids, bile acids, oxidative lipids, and aromatics were predominantly upregulated in M0 and M1, whereas lysophosphatidylcholines (LPCs), lysophosphatidyl ethanolamines (LPEs), and purines were primarily downregulated (Fig. S5B). Interestingly, we found contrasting changes in acylcarnitines (ACs) and hydroxyl ACs. ACs were downregulated, while hydroxyl ACs were upregulated. Furthermore, the levels of upregulated FAs, oxidative lipids, bile acids, and hydroxyl ACs were significantly higher in M1.

To further illustrate the trajectories of plasma metabolite levels during GC progression, the c-means clustering analysis [18] on the 264 discriminated metabolites were employed. We identified four distinct clusters (Figs. S5C and D in Supporting information). In the M0, the plasma metabolite levels in cluster 3 (ACs and nucleotides) and cluster 4 (aromatic compounds and carbohydrates) exhibited significant upregulation or downregulation but flattened out during the M1. This observation implies that metabolic vulnerabilities may emerge during specific early stages of tumor development. The plasma metabolite, particularly LPCs in cluster 1 and oxidative lipids and hydroxyl ACs in cluster 2, showed a consistent and gradual decrease or increase throughout the GC metastatic progression. This finding implies that these metabolites may be involved in the metabolic reprogramming associated with GC progression. Oxidative lipids are formed through the peroxidation of polyunstatured fatty acid (PUFAs) and result from an imbalance in the redox status and reactive oxygen species (ROS) accumulation [19]. A previous study reported that LPCs can exert their biological influence by stimulating cell division, releasing inflammatory factors, and inducing OS [20]. Consequently, the interplay between LPCs and oxidative lipids-associated OS may profoundly affect cancer progression and metastasis.

The circos plots revealed that inter-correlations among metabolites were significantly higher in M1 than in HC and M0 (Figs. 1D and E), implying that metabolic reprogramming is aggravated during tumor metastasis [11,21]. Furthermore, the metabolic pathways associated with caffeine, purine, sphingolipid, LPCs, and LPEs were significantly downregulated in M0 (Fig. 1C). Interestingly, the enrichment significance or abundance score showed no substantial alterations in cancer metastasis, implying that these metabolic pathways primarily contributed to GC genesis rather than metastasis. Linoleic acid metabolism, valine, leucine, and isoleucine biosynthesis, steroid metabolism, bile acid metabolism,

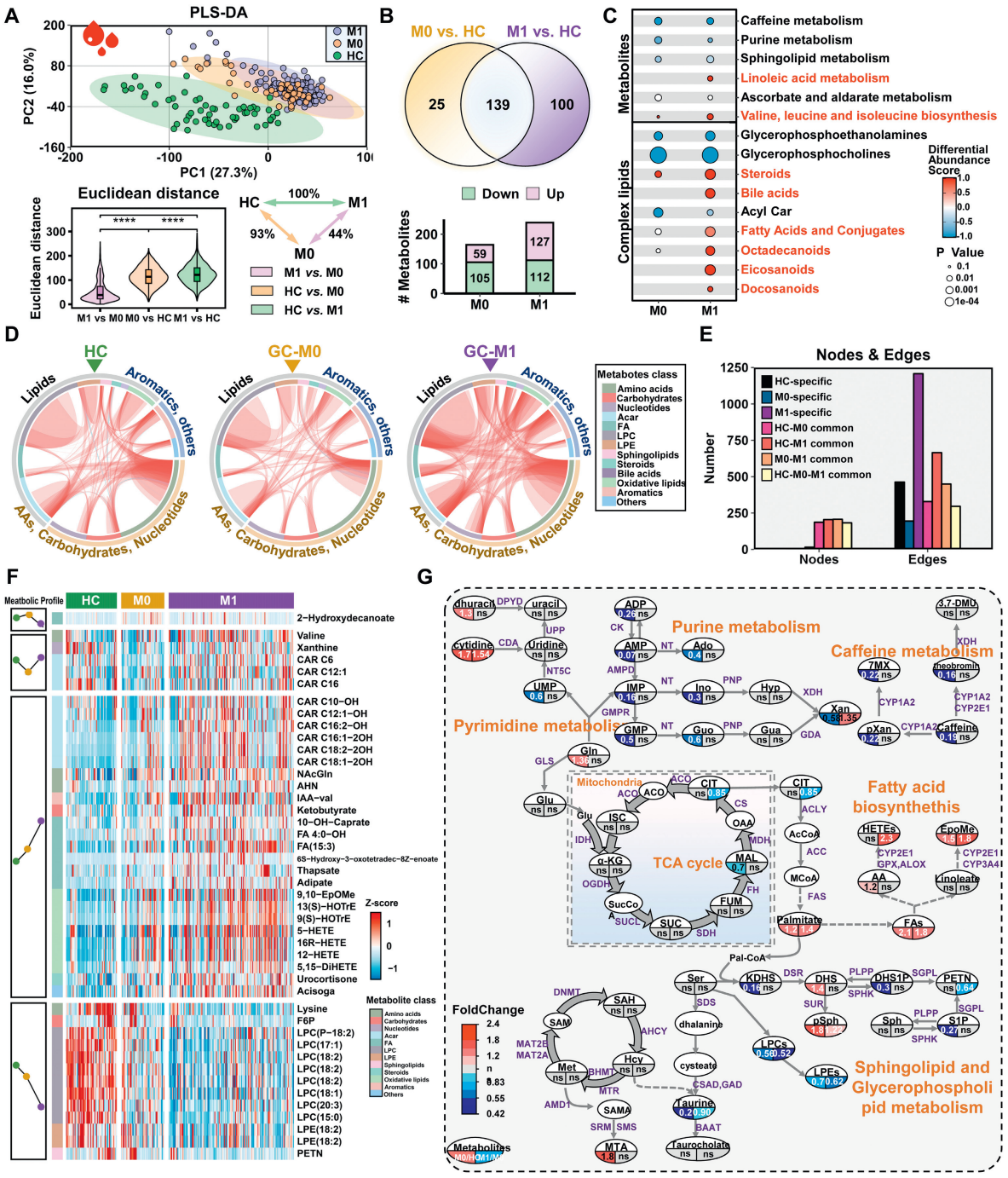

Fig. 1. Evolutionary metabolic alterations in circulating plasma of progressive GC. (A) PLS-DA analysis of the plasma metabolic expression profiles as well as their expression distances between the metabolic profiles of different groups, which were measured using Euclidean distances. The inset summarizes the average distance between pairs of samples as a percentage of the distance between M1 and HC plasma samples. ****$P < 0.001$. (B) Venn plot and bar plot of the differential metabolites in M0 (HC *vs.* M0) and M1 (HC *vs.* M1). (C) Metabolic pathways ($P < 0.05$) enriched by significantly differential metabolites in M0 (HC *vs.* M0) and M1 (HC *vs.* M1). (D) Circos plots of the differential metabolites ($P < 0.00001$). (E) Node and edge numbers in HC, M0, and M1 specific metabolic networks. (F) Heatmap of differential metabolites in plasma. (G) The integrated metabolic networks of GC. The full name of all the metabolites' abbreviations are summarized in the list of abbreviations in Supporting information.

eicosanoid metabolism, and docosanoid metabolism were significantly enriched in M1. The enrichment results suggest a positive correlation between the metabolic pathways and tumor metastatic progression. This finding was consistent with the heatmap profile of tumor metastasis-associated metabolites (Fig. 1F). Additionally, 45 metabolites were found to be differentially expressed between M0 and M1 ($P < 0.05$). The heatmap analysis revealed a continuous build-up of oxidative lipids and hydroxyl ACs derived from linoleic acid, linolenic acid, and arachidonic acid as GC progressed. Conversely, we observed a continuous decrease in LPCs that could be converted to linoleic acid, oleic acid, and eicosatrienoic acid. These results provide additional evidence of the involvement of PUFAs and their peroxidation in tumor metastatic progression. Furthermore, to present an in-depth view of the disrupted metabolic process in GC progression, we created a comprehensive metabolic atlas showing alterations in M0 and M1

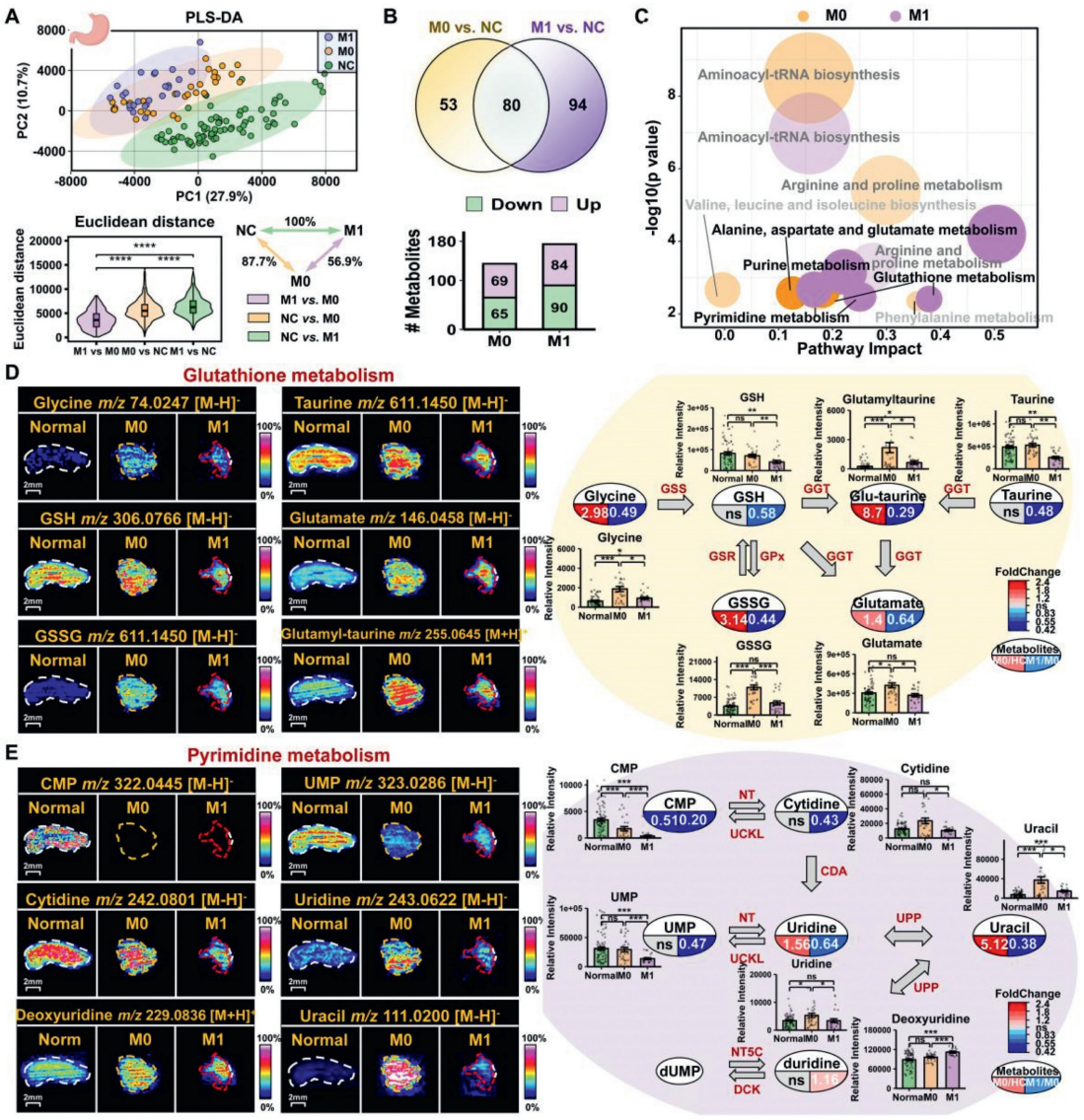

Fig. 2. Specific spatial metabolic alterations in progressive GC. (A) PLS-DA analysis of the metabolic expression profiles as well as their expression distances measured using Euclidean distances. The inset summarizes the average distance between pairs of samples as a percentage of the distance between M1 and NC tissue samples. $^{****}P < 0.001$. (B) Venn plot and bar plot of the differential metabolites with $P < 0.05$, and FC > 1.2 or FC < 0.833. (C) Significantly dysregulated metabolic pathways. MSI images and pathway networks of (D) glutathione metabolism and (E) pyrimidine metabolism.

(Fig. 1G), focusing primarily on purine and lipid metabolism disorders.

Highly spatially-resolved metabolomics analysis was performed using AFADESI-MSI to reveal the *in situ* tumor metabolic changes. The profile data pertaining to tissue micro-regions were effectively clustered into five distinct metabolic phenotypes through t-SNE spatial segmentation analysis (Figs. S6A and B in Supporting information). The analysis revealed significant variations in metabolite species and abundance across different tissue micro-regions (Figs. S6C and D in Supporting information). The PLS-DA analysis revealed notable differences in spatial metabolic profiles between tumor tissues and normal tissues. Euclidean distance between M1 and HC was significantly greater than that between M0 and HC or between M0 and M1 (Fig. 2A), indicating a progressive metabolic change tendency. Two-hundred and twenty-eight metabolites exhibited significant alterations in GCs, with 134 and 174 metabolites showing changes in M0 and M1, respectively (Fig. 2B). The higher number of specific discriminated metabolites in M1 tumors than in M0 indicates a more profound metabolic disorder in metastatic patients than non-metastatic patients, which aligns with findings from the aforementioned plasma metabolomics analysis. The disrupted metabolic pathways in both non-metastatic and metastatic GC by MetaboAnalyst showed that aminoacyl-tRNA biosynthesis, arginine and proline metabolism, purine metabolism, pyrimidine metabolism, and glutathione metabolism were the primary altered metabolic pathways (Fig. 2C). Furthermore, 133 metabolites exhibited significant alterations between M0 and M1 (Fig. S7A in Supporting information). These metabolites were predominantly enriched in pyrimidine metabolism, glutathione metabolism, and taurine and hypotaurine metabolism, all of which have been implicated in GC tumorigenesis and metastasis (Fig. S7B in Supporting information).

Glutathione metabolism and pyrimidine metabolism are the metabolic pathways that experienced the most significant dysregulation. glutathione (GSH) is critically involved in the body's antioxidant defense system and its glutathione metabolism maintains the body's redox balance. Fig. 2D illustrates the glutathione biosynthesis process involving glycine and γ-glutaminocysteine, followed

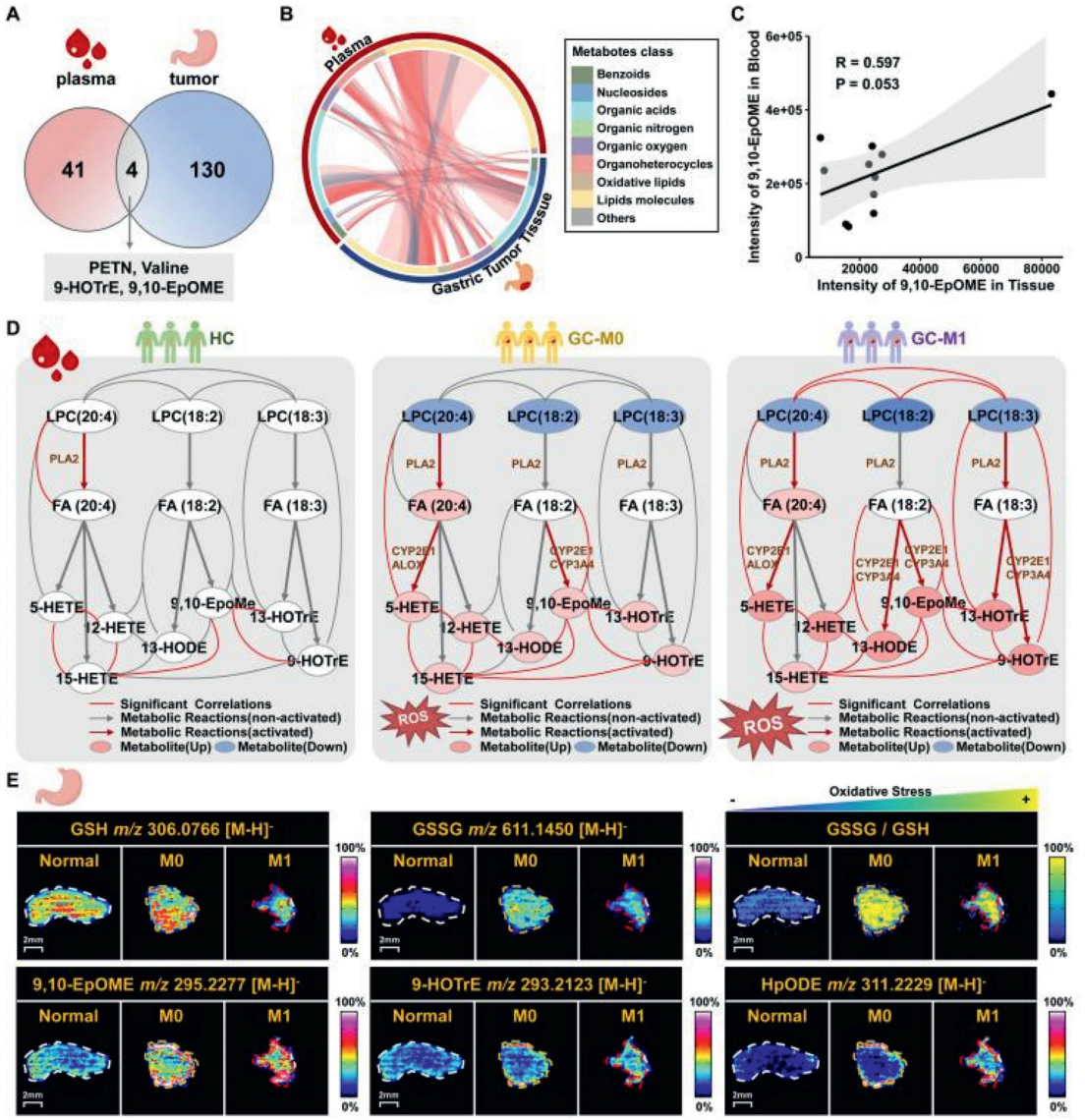

Fig. 3. Metabolic cross-talk of the oxidative lipids between tumor and plasma of GC. (A) Venn plot of the differential metabolites in tumor and plasma. (B) The circos plot of all metabolites' significant inter-correlations between plasma and tumor ($P < 0.005$). (C) The Pearson correlations of EpOMe in blood and tumor. (D) The metabolic pathway related to oxidative lipids in plasma. (E) AFADESI MS images of typical metabolites of oxidative metabolism in tissues.

by oxidation to oxidized glutathione (GSSG). Notably, GSSG can be reversed to GSH and GSH can be extracellularly transformed into γ-glutamylamino acids. In the glutathione metabolism pathway, it was observed that four metabolites (glycine, GSSG, glutamate, and glutamyl-taurine) were upregulated in M0 tumors, whereas five metabolites (GSH, glycine, GSSG, glutamate, and glutamyl-taurine) were downregulated in M1 tumors. This finding indicates a significant dysregulation in glutathione synthesis, oxidation, and extracellular excretion, potentially impacting the redox status of tumor cells. Furthermore, cancer development is closely associated with pyrimidine metabolism. Within the pyrimidine metabolism pathway (Fig. 2E), two metabolites (uridine and uracil) were upregulated in M0 tumors, while five metabolites (cytidine monophosphate (CMP), uridine 5′-monophosphate (UMP), cytidine, uridine, and uracil) were downregulated, indicating a dysregulation in pyrimidine biosynthesis.

An integrated analysis of plasma and spatially-resolved metabolomics were conducted from progressive GC patients to enhance the identification of metabolic crosstalk between tumor and plasma and investigate the underlying metabolic mechanisms. We identified four metabolites (phosphoethanolamine (PETN), valine, 9,10-epoxy-12-octadecenoic acid (9,10-EpOMe), and 9-hydroxyoctadeca-10,12,15-trienoic acid (9-HOTrE)) changed with the same trend in both tumor and plasma (Fig. 3A). Their structures were shown in Fig. S8 (Supporting information), encompassing two oxidative lipid species. We further investigated the metabolic correlations among the discriminated metabolites in tumor tissues and plasma (Fig. 3B). Notably, 9,10-EpOMe (a class of the oxidative lipids derived from linoleic acids) exhibited a significantly positive correlation between tumor tissues and plasma ($P = 0.053$, $R = 0.593$) (Fig. 3C). These findings highlight the active involvement of oxidative lipids in metabolic communication between GC tumors and the bloodstream, which might be crucial in the metabolic reprogramming of tumorigenesis and metastasis.

The metabolic pathway related to oxidative lipids was further investigated. As shown in Fig. 3D, a specific metabolic network that showed correlations between the differential metabolites (LPCs, PUFAs, and oxidative lipids) was discovered in plasma. For instance, LPC (18:2), LPC (18:3), and LPC (20:4) can be hydrolyzed into FA (18:2), FA (18:3), and FA (20:4), which subsequently un-

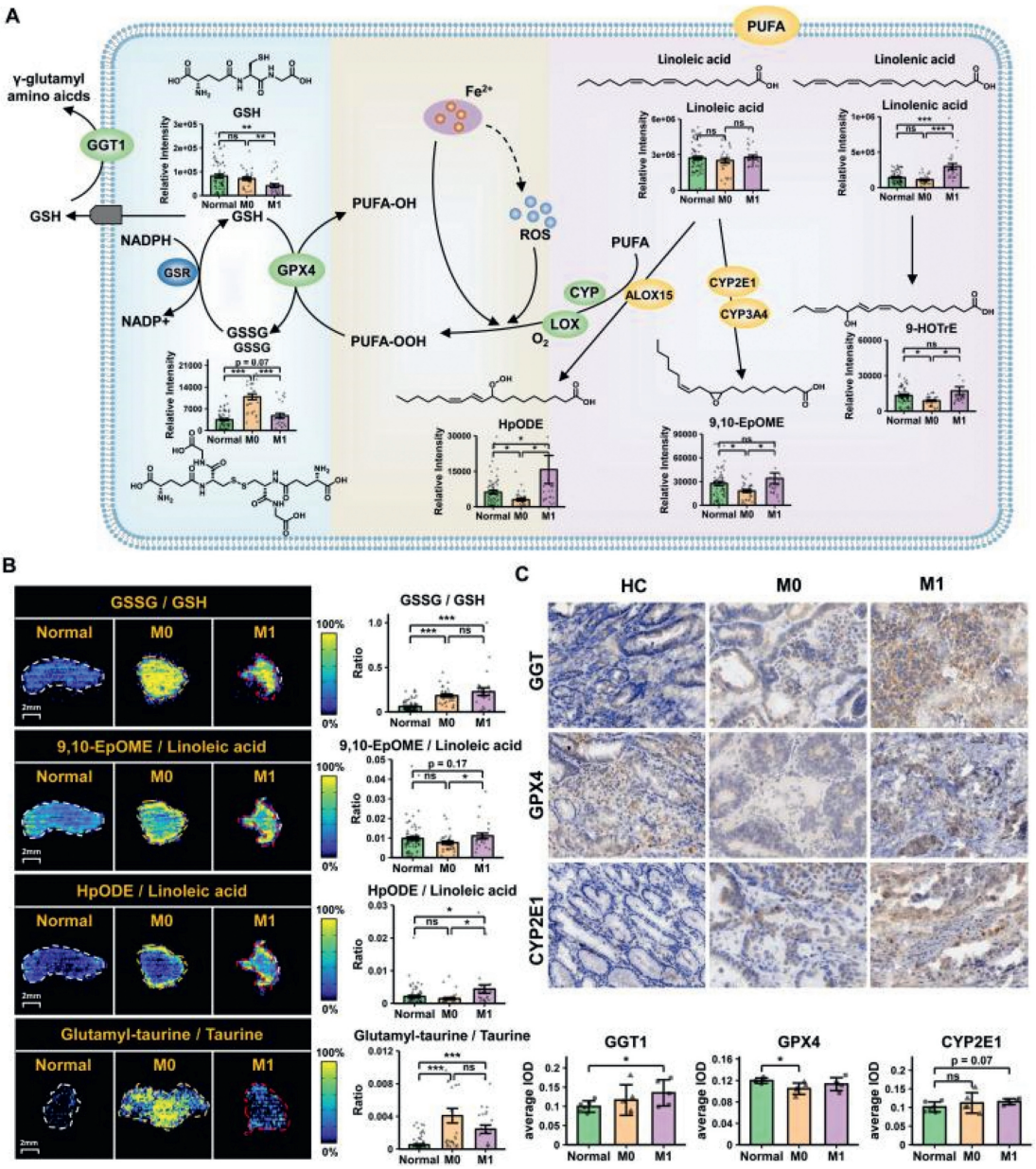

Fig. 4. *In situ* discovery and validation of altered metabolic enzymes in oxidative lipids pathways. (A) Metabolic pathway of glutathione and oxidative lipids in the tumor cells. (B) The newly constructed MS image and statistical results based on the ion-intensity ratio of GSSG to GSH, 9,10-EpOMe to linoleic acid, HpODE to linoleic acid, and glutamyl-taurine to taurine. (C) Expression of enzyme GGT1, GPX4, and CYP2E1 in different tissues by immunohistochemistry staining.

dergo peroxidation to form various oxidative lipids, such as 5-hydroxyeicosatetraenoic acid (5-HETE), 9-HOTrE, 9,10-EpOMe. By comparing the inter-correlations among plasma metabolites in HC, M0, and M1, we found that the correlational activity of the oxidative lipids metabolic network became increased in M0, and was even aggravated in M1.

Moreover, the MSI analysis revealed that GSH were depleted in M1 tumors, whereas GSSG accumulated in both M0 and M1 tumors (Fig. 3E and Fig. S9 in Supporting information). Hence, the GSSG/GSH ratio in normal tissues had an average ratio of only 0.06. However, this ratio tended to dramatically increase in M0, reaching a ratio of 1:1. While, it was not statistically significant in M1 compared with M0. The dynamic balance and interconversion of GSH and GSSG play a crucial role in the assessment of the redox status of cells and tissues [19,22]. This observation is consistent with the upregulated the expression of PUFA and its oxidative metabolites in M0 and M1 tissues, such as linoleic acid, 9,10-EpOMe, HOTrE, and hydroperoxyoctadecadienoic acid (HpODE).

Thus, the integrative analysis of plasma metabolomics and tumor metabolomics both revealed a significant increase in the redox imbalance and high oxidative stress, and then the lipid peroxidation of poly-unsaturated fatty acids in the body of GC patients experiencing tumorigenesis and metastasis. The transcriptome expression profile of mRNA markers associated with oxidative stress in gastric tumor tissues from an independent the Cancer Genome Atlas (TCGA) GC cohort ($n = 340$) further confirmed the validity of our findings (Fig. S9).

The MSI and immunohistochemistry (IHC) [15,23] were utilized to identify potential tumor-associated metabolic enzymes involved in oxidative lipids metabolism in GC. The present findings indicate a significant increase in the ratios of GSSG to GSH, 9,10-EpOME to linoleic acid, HpODE to linoleic acid, and glutamyl-taurine to tau-

rine in M0 or M1 tumors (Fig. 4B). Fig. 4A summarized that linoleic acid and linolenic acid can be oxidized through the catalyzation of CYP and LOX enzymes [24-26]. This implies that there might be abnormal expression of GPX4, GSR, CYP2E1, CYP3A4, ALOX15, and GGT1 in tumors. By further investigating with IHC semi-quantitative analysis, the results shown in Fig. 4C indicate that GPX4 is underexpressed in M0. Additionally, GGT1 is significantly upregulated in M1. CYP2E1 is slightly overexpressed in M1, which could explain the increase of 9,10-EpOMe to a certain extent. Studies have shown that the accumulation of ROS causes metabolic reprogramming in tumors [19]. Thus, we further performed log-rank survival analysis of CYP2E1 mRNA and GGT1 mRNA expression via the public TCGA database. The results demonstrated that high expression of CYP2E1 and GGT1 were significantly correlated with the clinical outcomes of GC patients (Fig. S11 in Supporting information), which further confirmed the potential effect of CYP2E1 and GGT1 in GC metastasis.

Therefore, our findings suggest that the upregulation of GGT1 in GC tumors may cause a significant decrease in GSH and increase in the ratio of GSSG to GSH. The shift in redox metabolism and the resulting surge in oxidative stress contribute to the tumorigenesis of GC. Furthermore, the increase in oxidative stress, coupled with a slight upregulation of CYP2E1, enhances the peroxidation of poly-unsaturated fatty acids as the disease progress, especially at GC metastasis. This is evidenced by the increased expression of oxidative metabolites of PUFA, including 9,10-EpOMe, HOTrE, HpoDE, among others.

An integrative metabolomics approach was proposed in this study to characterize the global metabolic landscape of plasma and tissue samples of GC using LC–MS- and AFADESI-MSI-based metabolomics. Compared with the traditional metabolomics approach, this integrative metabolomics strategy could provide comprehensive detection of metabolites and reveal spatial metabolic information of tumor tissue microregions as well as the metabolic information of the blood system, thereby characterize the global metabolic atlas. Furthermore, using the integrative metabolomics approach have discovered metabolic communications of lipid peroxidized metabolites of poly-unsaturated fatty acids between tumors and blood. In addition, through data-driven MSI ratio analysis and IHC analysis, we obtained further evidence regarding the activation of oxidative lipid metabolism and increased oxidative stress during the progression of gastric cancer. This multi-dimensional dataset elucidated the extensive metabolic changes occurring during the metastatic progression of GC. It offers valuable insights for investigating the dynamic metabolic responses of advanced GC patients to this progression. However, there are some limitations to this study. Experiments on animal models would be conducting for delving into the potential underlying mechanisms.

Declaration of competing interest

The authors declare that they have no known competing financial interests or personal relationships that could have appeared to influence the work reported in this paper.

CRediT authorship contribution statement

Yanhua Chen: Writing – review & editing, Writing – original draft, Supervision, Project administration, Methodology, Investigation, Funding acquisition, Formal analysis, Conceptualization. **Xian Ding:** Writing – original draft, Software, Investigation, Methodology, Formal analysis, Data curation. **Jun Zhou:** Resources, Conceptualization. **Zhaoying Wang:** Methodology, Funding acquisition. **Yunhai Bo:** Resources. **Ying Hu:** Resources. **Qingce Zang:** Methodology. **Jing Xu:** Methodology. **Ruiping Zhang:** Methodology. **Jiuming He:** Methodology. **Fen Yang:** Validation, Supervision, Investigation, Funding acquisition, Conceptualization. **Zeper Abliz:** Supervision, Project administration, Funding acquisition.

Acknowledgments

The authors thank the financial support from the National Key R&D Program of China (No. 2022YFC3401003), the National Natural Science Foundation of China (Nos. 21927808, 82073817, 22104160). We thank the Peking University Cancer Hospital Biobank, for use of its facilities and services, and thank the participants of the study, and all clinical and research staff who contributed to the study.

Supplementary materials

Supplementary material associated with this article can be found, in the online version, at doi:10.1016/j.cclet.2024.110351.

References

[1] H. Sung, J. Ferlay, R.L. Siegel, et al., CA Cancer J. Clin. 71 (2021) 209–249.
[2] E. Morgan, M. Arnold, M.C. Camargo, et al., eClinicalMedicine 47 (2022) 101404.
[3] E.C. Smyth, M. Moehler, Ther. Adv. Med. Oncol. 11 (2019), doi:10.1177/1758835919867522.
[4] M.Z. Qiu, S.M. Shi, Z.H. Chen, et al., Cancer Med. 7 (2018) 3662–3672.
[5] W. Yasui, N Oue, P.P. Aung, et al., Gastric Cancer 8 (2005) 86–94.
[6] K. Ganesh, J. Massague, Nat. Med. 27 (2021) 34–44.
[7] P. Bu, K.Y. Chen, K. Xiang, et al., Cell Metab. 27 (2018) 1249–1262 e4.
[8] A.P. Gomes, D. Ilter, V. Low, et al., Nature 585 (2020) 283–287.
[9] Y.Z. Chen, B.H. Wang, Y.Z. Zhao, et al., Nat. Commun. 15 (2024) 1657.
[10] X.X. Wang, B.L. Wang, F.F. Ji, et al., Chin. Chem. Lett. 35 (2024) 109653.
[11] B. Faubert, A. Solmonson, R.J. DeBerardinis, Science 368 (2020) eaaw5473.
[12] U.E. Martinez-Outschoorn, M. Peiris-Pages, R.G. Pestell, et al., Nat. Rev. Clin. Oncol. 14 (2017) 11–31.
[13] A. Tasdogan, B. Faubert, V. Ramesh, et al., Nature 577 (2020) 115–120.
[14] C.L. Sun, T.G. Li, X.W. Song, et al., Proc. Natl. Acad. Sci. U. S. A. 116 (2019) 52–57.
[15] J.P. Huang, S.S. Gao, K. Wang, et al., Chin. Chem. Lett. 34 (2023) 107865.
[16] X. Ding, F. Yang, Y.H. Chen, et al., Anal. Chem. 94 (2022) 7500–7509.
[17] C.L. Sun, A.Q. Wang, Zhou Y.H, et al., Nat. Commun. 14 (2023) 2692.
[18] L. Kumar, M.E. Futschik, Bioinformation 2 (2007) 5–7.
[19] G. Barrera, ISRN Oncol. 2012 (2012) 137289.
[20] P. Liu, W. Zhu, C. Chen, et al., Life Sci. 247 (2020) 117443.
[21] K. Ohshima, E. Morii, Metabolites 11 (2021) 28.
[22] V. Chiurchiu, A. Leuti, M. Maccarrone, Front Immunol. 9 (2018) 38.
[23] S. Enya, K. Kawakami, Y. Suzuki, et al., Dis. Model Mech. 11 (2018) dmm032383.
[24] K. Strassburg, A.M.L. Huijbrechts, K.A. Kortekaas, et al., Anal. Bioanal. Chem. 404 (2012) 1413–1426.
[25] H. Bayir, T.S. Anthonymuthu, Y.Y. Tyurina, et al., Cell Chem. Biol. 27 (2020) 387–408.
[26] S. Doll, M. Conrad, IUBMB Life 69 (2017) 423–434.